Journal of Physics: Conference Series

PAPER • OPEN ACCESS

Experimental study of a phase change material storage for low-temperature applications

To cite this article: G Besagni and L Croci 2020 *J. Phys.: Conf. Ser.* **1599** 012003

Experimental study of a phase change material storage for low-temperature applications

G Besagni[1] and L Croci[1]

[1] Power System Development Department, Ricerca sul Sistema Energetico - RSE S.p.A., via Rubattino 54, Milano, 20134, Italy
Corresponding author e-mail: giorgio.besagni@rse-web.it

Abstract. Thermal energy storage technologies are matter of intense research and discussion, in the broader framework of decoupling the "demand-side" and the "supply-side". This topic is of paramount importance to support the large-scale deployment of renewable energy-based technologies in the residential sector, to support the decarbonisation pathways. In this perspective, a promising solution concerns solar-assisted heat pumps. This paper contributes to the existing discussion by developing, building and testing a "pilot-scale" finned-and-tube phase change material storage for solar-assisted heat pumps applications (viz.,low temperature applications, in the range of 20 - 30 °C). The proposed storage unit is tested, under real boundary conditions and it is able to store 65 % higher thermal energy stored compared with an equivalent water storage unit.

1. Introduction

Modifying the equilibrium point between the so-called "*demand-side*" and the "*supply-side*" of the household sector is of paramount importance to achieve the demand-side management. Such goal can be obtained by using thermal and electrical energy storages; this paper contributes to the existing discussion on thermal energy storages for solar-assisted heat pumps (viz., storage temperatures in the range of 23 - 29 °C, ref. [1]). Indeed, the deployment of heat pumps in the household sector is a widely accepted preferential path for the decarbonisation of country energy system [2]. Unfortunately, the performances of solar-assisted heat pumps are related to the availability of the solar source and, thus, a storage unit is needed to boost their efficiency [1]. Among the storage technologies reviewed by Zhang et al. [3], PCM-based systems are of particular interest, owing to the high energy storage density within a narrow temperature range [4]. Unfortunately, the application of PCM-based systems is hindered by the low thermal conductivity: despite some heat transfer enhancement methods were proposed, an agreement is still elusive. In this framework, the use of finned tubes heat exchanger (based on commercially available heat exchangers) is attracting a growing interest [5-9]. Despite these studies provided valuable and interesting results, it is recognized the need of "*pilot-scale*" studies to clarify the system behaviour under relevant operating conditions. Given the state-of-the-art, this paper contributes to the present discussion by proposing and testing a novel pilot-scale phase change materials storage unit for solar-assisted heat pumps. The proposed storage has been tested by using an ad-hoc developed test ring. The remaining of the article is organized as follows. Section 2 discussed the experimental setup, methods and performance criteria; Section 3 discusses the experimental observations and, finally, the concluding remarks are provided within Section 4.

2. Experimental setup and methods

2.1. The test ring

Figure 1 and Table 1 display the test ring, the system components and instrumentation data. A reversible heat pump imposes the cooling loads by maintaining the "*buffer storage tank*" at 15 °C. Subsequently, the "*buffer storage tank*" is connected to the *PCM* storage by an hydraulic circuit, having a plate heat exchanger as well as a deviation valve. A variable speed pump imposes the propylene-water-glycol mixture flow rate and two electrical resistances impose the heating load (P_{el}). All pipes and system components were insulated to avoid thermal losses. It is worth noting that the temperature probes were verified with a calibration prior to experimentation.

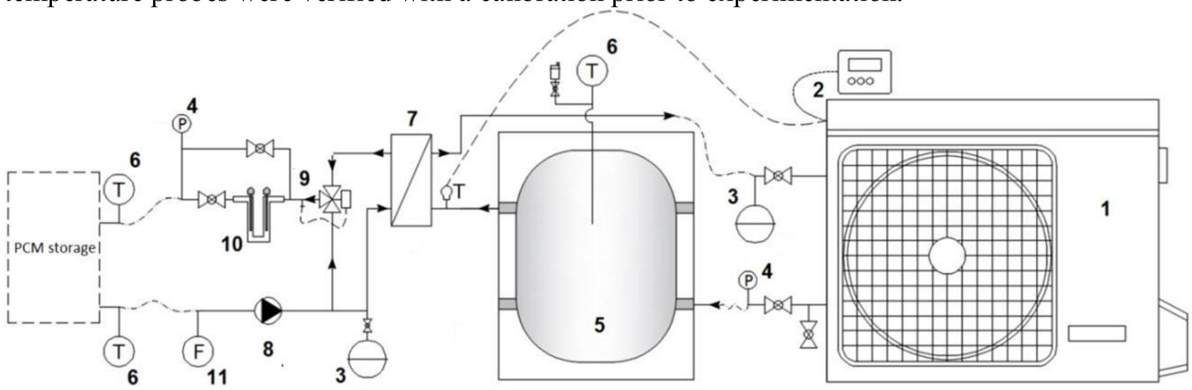

Figure 1. The experimental setup.

Table 1. Details of the system components displayed in Figure 1.

Code name	Equipment	Uncertainties
1	Reversible heat pump (MAXA, i-HWAK//V4 06, R410A)	--
2	Remote control system for the reversible heat pump	--
3	8dm^3 expansion tank	--
4	Pressure Transducer	±0,5% r.v
5	Buffer storage tanks for heat pumps; 51l, water storage (*volano termico PdC50 manufactured by Cordivari*)	--
6	Temperature probe - RTD Pt100 (1/5DIN)	±0,06 °C (0 °C)
7	Plate heat exchanger (*SLB20 manufactured by Cordivari*)	--
8	Variable speed circulation pump (EB Evolplus Small 60/180 M PWM, power: 5 ÷ 100 W)	--
9	Deviation valve (*comparato Nello Diamix Pro*)	--
10	Two electrical resistances (2x1500 W)	--
11	Electromagnetic flow meter (Promag DN15 *manufactured by Endress & Hauser*)	±0,2% r.v

2.2. The storage unit

The proposed storage unit is based on a fin-and-tube heat exchanger (in agreement with ref. [9]) surrounded by PCM material and placed within an external tank (insulated by a 60 mm polystyrene layer and covered by a reflective material). Given the experimental observations in ref. [1] (the system is supposed to work within the range of 23-29 °C), 58 kg of RT26 (manufactured by Rubitherm GmbH) was used to fill the storage unit. RT26 is a paraffin having the following properties: (a) specific heat capacity equal to 2 kJ/kg K; (b) melting/congealing temperature in the range of 25-26 °C (peak at 26 °C), (c) heat storage capacity equal to 180 kJ/kg, (d) solid density equal to 880 kg/m^3, (e) liquid density equal to 750 kg/m3, (f) heat conductivity equal to 0.2 W/m K. The heat exchanger is composed by 4 hydraulic circuits, connected by an external manifold (allowing testing the storage unit in both parallel and series configurations), aluminum fins (3 mm pitch, 0.25 mm thickness) and 12 tubes (14 mm inner diameter). 3 temperature probes (RTD Pt100 Class A, ±0,15 °C at 0 °C - T_1, T_2, T_3) were placed at different locations (Figure 2) to monitor the local temperatures; their locations have been selected to describe the local phenomena between the fins as well as in the lateral regions. Future studies will be devoted to include additional thermocouples to ensure a comprehensive study.

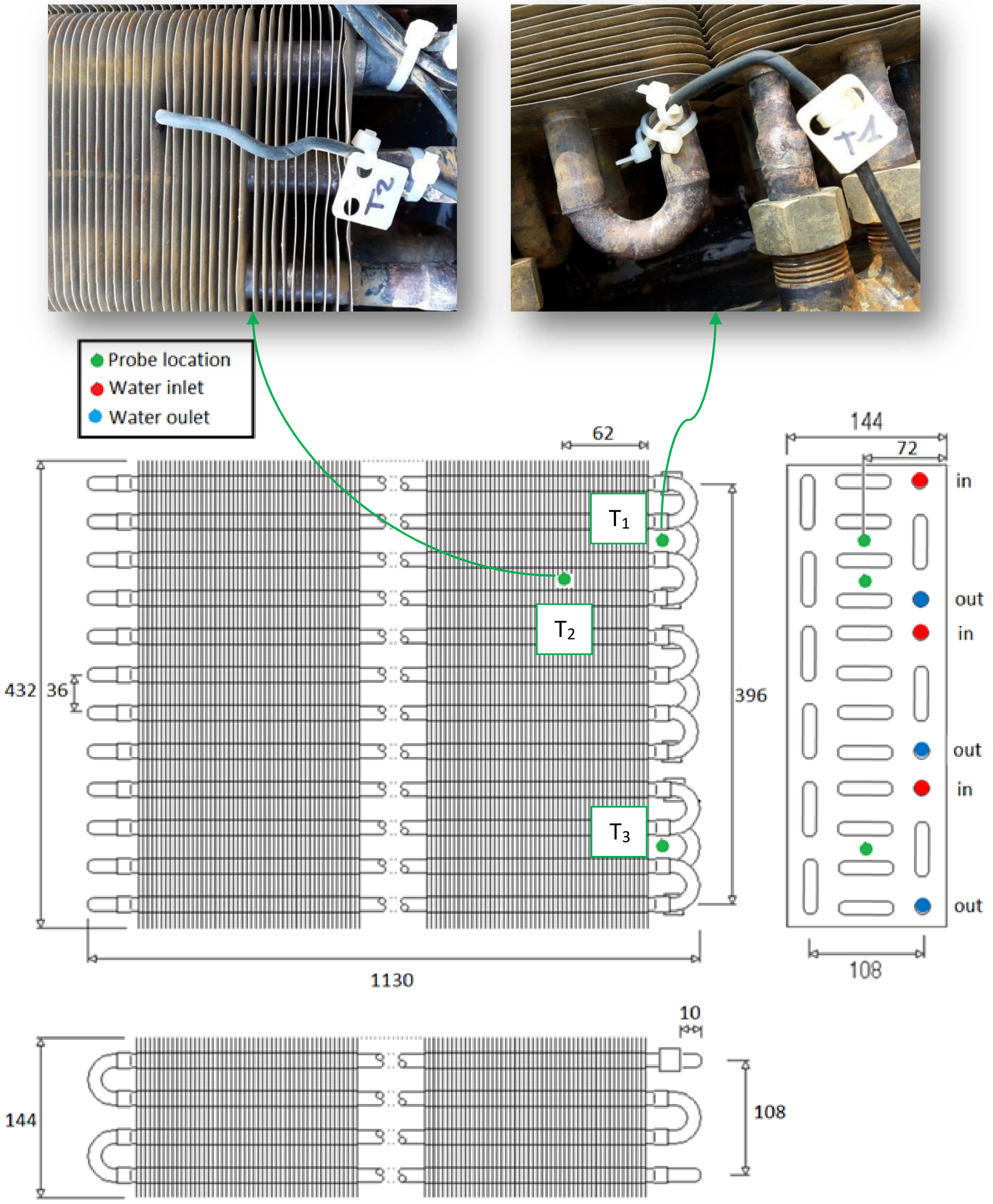

Figure 2. Details of storage system: system design (measurements in [mm]), inlet and outlet location of the water flowing within the heat exchanger, RTD Pt100 temperature probe locations and corresponding photos.

2.3. Performance parameters and tested cases

Storage unit charge/discharge energy (E_{th}) is computed as the integral of the instantaneous power ($\dot{Q}$), based on the energy balance on the water-side, assuming an adiabatic process (verified by preliminary observations, see Figure 3, where is noted that heat losses of the system can be considered negligible, given the practical application and operation modes of the storage unit):

$$\dot{Q} = \dot{m}c_p(T_{in} - T_{out}) = \dot{V}\rho c_p(T_{in} - T_{out}) \quad (1)$$

$$E_{th} = \sum_{t=0}^{t=endTime} \dot{Q} \tag{2}$$

Where t is the temporal variable. Finally, the parameter UA is computed following the proposal of Palomba et al. [9]:

$$UA = \dot{Q} / \left(T_{average} - \frac{T_{in} + T_{out}}{2} \right) \tag{3}$$

Where $T_{average}$ is the mean temperature within the storage unit, computed as the mean value between T_1, T_2 and T_3.

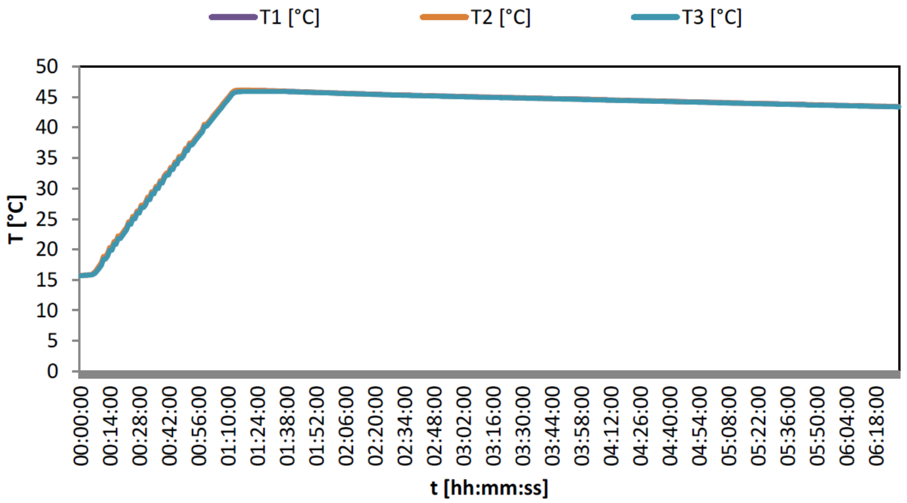

Figure 3. Preliminary test to check heat losses (storage unit filled with water).

2.4. Performance parameters and tested cases

Prior to the experimentation, a pre-conditioning of the storage is obtained, by setting the storage unit at constant temperature (15 °C). Subsequently, the charge phase is started. In this phase, the electrical resistances are switched on at constant power and the flow rate is circulated at $V_{heating}$. The resistances are switched off when $T_{average}$ (viz., the mean temperature within the storage unit, computed as the mean value between T_1, T_2 and T_3) is equal to $T_{heating}$; finally, the flow rate is circulated at $V_{heating}$ till T_{in}, T_{out}, T_1, T_2 and T_3 reach the same temperature and keep it constant for 5 minutes. At this point, the discharge operation is started. In this phase, valve (*#4*, Figure 1) is operated to connect the right and left sides of the facility (Figure 1), and the flow rate is circulated at $V_{cooling}$ till T_1, T_2 and T_3 reach 15 °C (it should be noted that the heat pump maintains the temperature of the buffer storage at 15 °C, thus acting as an heat sink). This procedure was applied to the cases listed in Table 2; please note that in the test matrix, water has been included to clarify the influence of the storage material employed.

Table 2. Test matrix.

Code name	Configuration	Test settings
WATER	Parallel	$P_{el} = 1.3kW$, $T_{heating} = 35°C$ $V_{heating} = 370m^3/h$, $V_{cooling} = 430m^3/h$
PCM 1	Parallel	$P_{el} = 1.3kW$, $T_{heating} = 35°C$ $V_{heating} = 370m^3/h$, $V_{cooling} = 430m^3/h$
PCM 2	Series	$P_{el} = 1.3kW$, $T_{heating} = 35°C$, $V_{heating} = 370m^3/h$, $V_{cooling} = 370m^3/h$

3. Results and discussion

This section discusses the experimental results. First, repeatability testes are presented; secondly, the influence of the storage material is discussed and, third, the influence of the heat exchanger configuration is outlined

3.1. Repeatability tests

Figure 4 and Figure 5 display the results of the repeatability tests for both the parallel ("*PCM 1*") and series configurations ("*PCM 2*"). The heating phases show minimum deviations; conversely, the cooling phases show a larger variability (probably owing to the flow distribution imposed by the valve). Given the outcome of this study (testing a pilot scale systems under relevant operating conditions), the present outcomes might be considered acceptable.

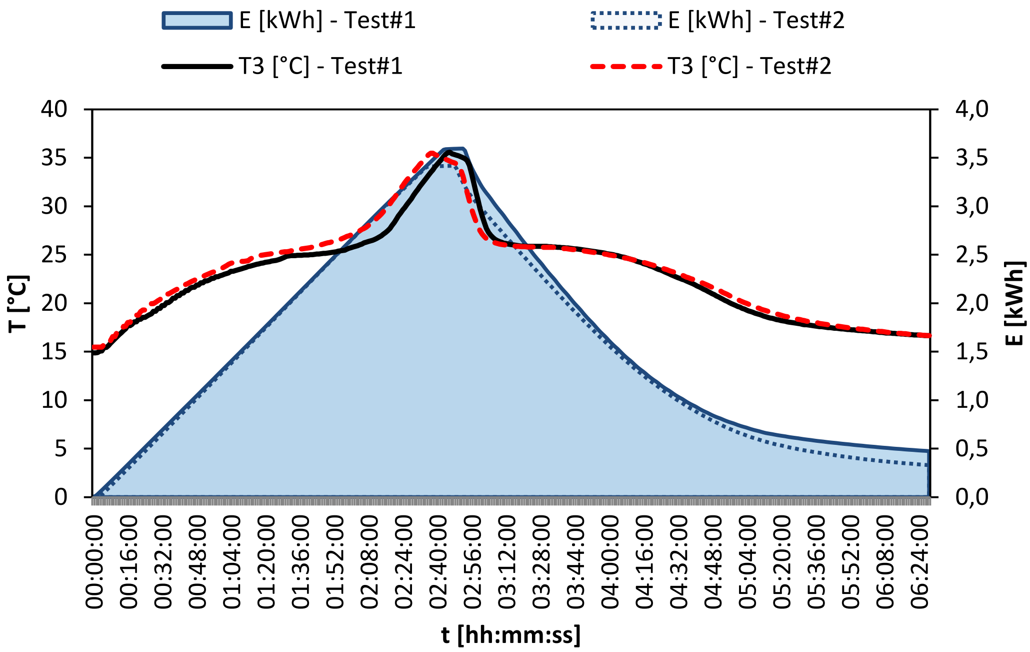

Figure 4. Repeatability tests: instantaneous profiles of temperatures and thermal energy in the parallel configuration.

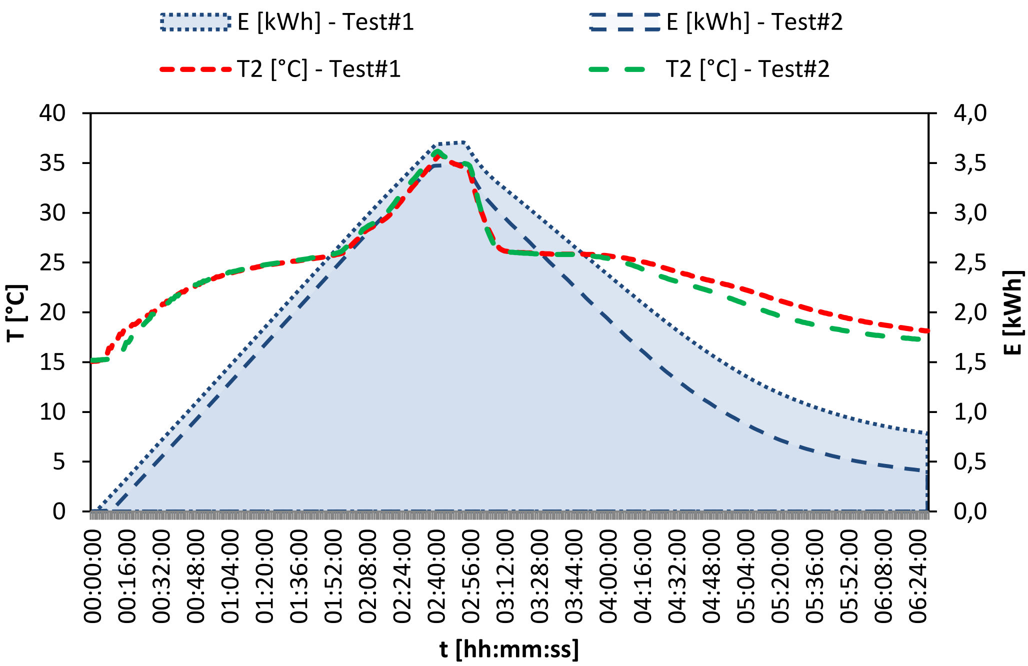

Figure 5. Repeatability tests: instantaneous profiles of temperatures and thermal energy in the series configuration

3.2. Comparison with water

Figure 6 compares the water test with "*PCM 1*" and "*PCM 2*" tests in terms of instantaneous quantities. It is observed that "*PCM 1*" case is able to store 65 % higher thermal energy compared with water storage media. Such value is also higher compared with the value observed in ref [9] (50 %): this outcome is very interesting and support the suitability of the proposed design criteria. In the "*Water"* case, *UA* is in the range of 600 W/K (in the heating mode) and 900 W/K (in the cooling mode); conversely, in the "*PCM 1" and "PCM 2"* cases, *UA* is in the range of 400-500 W/K (in the heating/cooling modes). These differences support the discussion regarding the limitations of the heat transfer process given by the lower thermal conductivity of *PCM* compared with water (as expected based on the previous literature on *PCM* properties, [9]). It should be noted that the range of values of *UA* are higher compared with the ones reported by Palomba et al. [9] (100 W/K), supporting the correct design of the proposed storage unit.

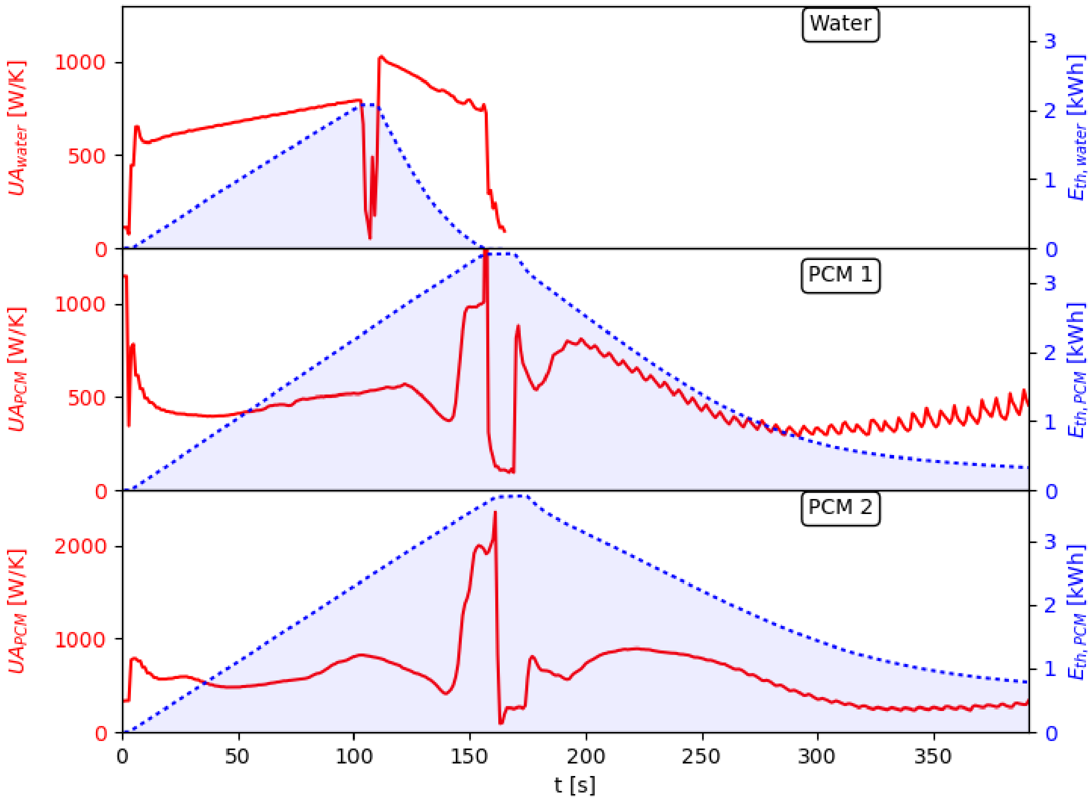

Figure 6. Effect of the storage material on instantaneous E_{th} and UA measurements: comparison between "Water" (sensible storage) and "*PCM 1*" (latent/sensible storage) cases.

3.3. Comparison between the different heat exchanger configurations

Figure 7 ("*PCM 1*" – parallel configuration) and Figure 8 ("PCM 2" – series configuration) compare the "*PCM 1*" and "*PCM 2*" tests in terms of local and instantaneous quantities. Regardless of the heat exchanger configuration, all curves are characterized by similar shapes. During *phase#1*, T_{in} increases because of the thermal power supplied to the circulating water and, consequently, T_{out} increases. Subsequently T_1, T_2 and T_3 increase, owing to the thermal power provided to the *PCM* by the heat exchanger. Looking closer at the internal temperatures (T_1, T_2, T_3) three sub-phases are identified: (i) solid-phase sensible heating; (ii) phase change in the range of 25 – 26 °C (as expected from the *PCM* datasheet and properties); (iii) liquid-phase sensible heating until $T_{heating}$. Subsequently, the thermal energy is removed from the storage units, by acting on the deviation valve, and the internal temperatures decrease. The cooling phase is specular for the heating phase. It is worth noting that T_2 is higher than T_{out} in the charge phase and lower than T_{out} in the discharge phase in both the series and the parallel configuration. Such values are likely to be explained by non-uniform heat transfer process within the heat exchanger and by the large-scale dimensions of the systems, thus leading to a non-uniform heating/cooling. Future studies will be devoted to include additional thermocouples to ensure a comprehensive study regarding non-uniformities.

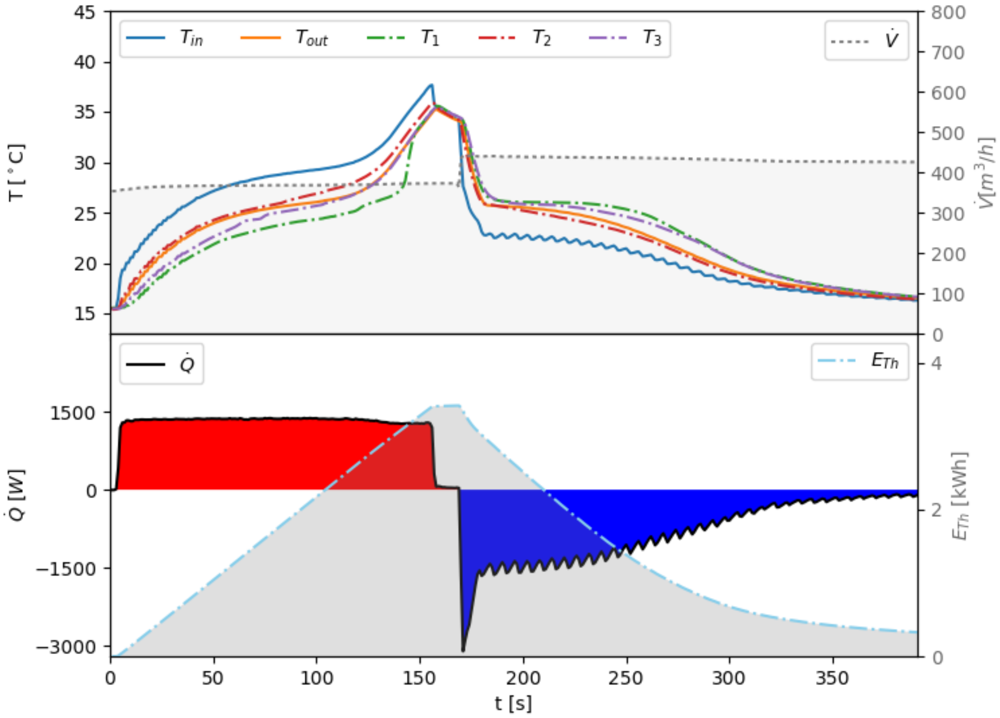

Figure 7. Instantaneous profiles of temperatures, power supplied/removed and thermal energy – Case "*PCM 1*" (see Table 2 for further details on the case).

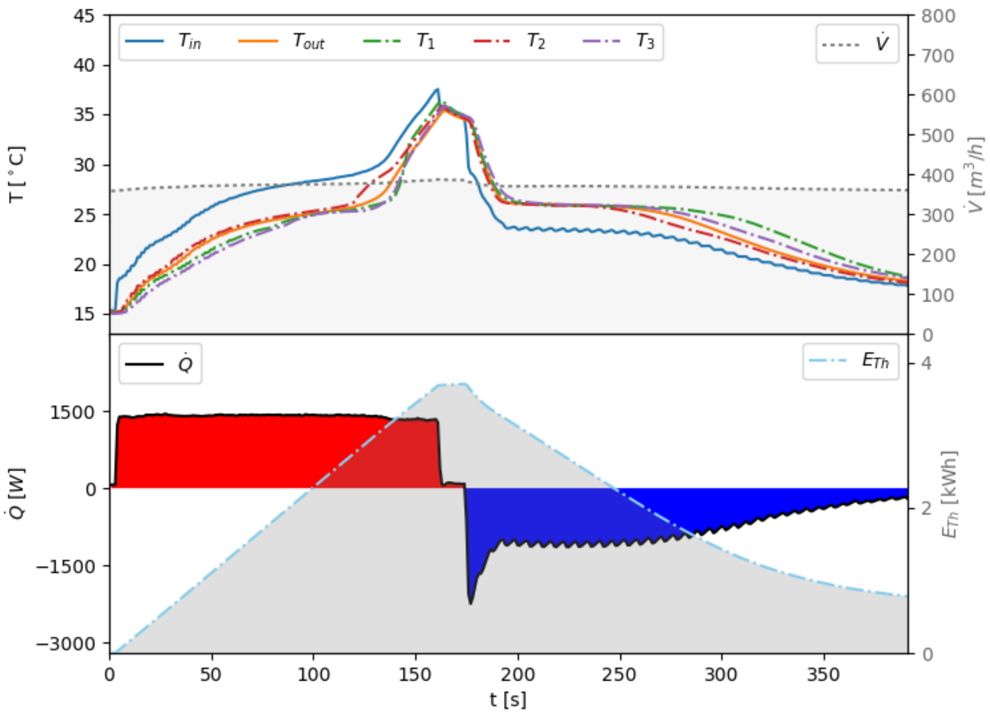

Figure 8. Instantaneous profiles of temperatures, power supplied/removed and thermal energy – Case "*PCM 2*" (see Table 2 for further details on the case).

The influence of the heat exchanger configurations (parallel or series) can be commented by taking into consideration the locations of the temperature probes. In the parallel configuration (Figure 7), a difference in T_1 and T_3 is noted during the charging phase besides, in the cooling phase, the duration of phase change at location #1 (Figure 2) takes a longer period and appears more stable. This difference might be caused by a hydraulic maldistribution at the heat exchanger inlet. As expected, the central part of the heat exchanger (location #2 in Figure 2) has higher melting rate and shows higher temperatures compared with the other probes. In the series configuration (Figure 8), the difference between the values of T_1 and T_3 is lower compared with the parallel configuration; on the other hand, the cooling phase in the series mode is similar to the parallel configuration. The duration of the heating phase in both configurations is similar, whereas the duration in the cooling mode in the series configuration is higher, possibly owing to the lower flow rate.

4. Conclusion

This paper contributes to the existing discussion on thermal storage systems by developing a “pilot-scale” finned and tube phase change material storage to support the deployment of solar assisted heat pumps. The *PCM*-based storage units was developed and tested under real boundary conditions, showing 65 % higher energy compared with a water storage. This outcome is very interesting in the deployment of solar assisted heat pumps and the integration between the present storage unit and heat pumps systems will be carried on in the forthcoming research activities. Subsequently, the storage unit was tested in two different heat exchanger configurations (parallel or series) and the results were critically analyzed based on the local measurements. In addition, the obtained dataset poses a valuable basis to validate numerical codes.

5. References

[1] Besagni G, Croci L, Nesa R and Molinaroli L 2019 Renew Energ 132 1185-1215
[2] Buker M and Riffat S B 2016 Renew Sust Energ Rev 55 399-413
[3] Zhang H, Baeyens J, Cáceres G, Degrève J and Lv Y 2016 Prog Energ Comb 53 1-40
[4] Mehling H and Cabeza L F 2008 Heat and cold storage with PCM - An up to date introduction into basics and applications Springer-Verlag Berlin Heidelberg
[5] Medrano M, Yilmaz M O, Nogués M, Martorell I, Roca J and Cabeza L F 2009 Appl Energ 86 2047-2055
[6] Agyenim F, Eames P and Smyth M 2009 Sol Energy 83 1509-1520
[7] Eslamnezhad H and Rahimi A B 2017 Appl Therm Eng 113 813-821
[8] Acır A and Canlı M E 2018 Appl Therm Eng 144 1071-1080
[9] Palomba V, Brancato V and Frazzica A 2017 Appl Energ 347-358

Acknowledgments

This work has been financed by the Research Fund for the Italian Electrical System in compliance with the Decree of Minister of Economic Development April 16, 2018.